

Cite this: *RSC Sustainability*, 2025, 3, 4126

# A more sustainable two-step synthesis of alkylated $\beta$ -cyclodextrin via acetylation and $\text{GaBr}_3$ -catalyzed reduction

Leon J. Bartlewski,<sup>a,b</sup> Peter Conen,<sup>a,b</sup> Qianyu Cai,<sup>b</sup> Maximilian Bürk,<sup>b</sup> Dominique Armspach,<sup>c</sup> and Michael A. R. Meier<sup>\*a,b</sup>

Cyclodextrins (CDs) are bio-based and biodegradable oligosaccharides, enzymatically derived from starch, offering low toxicity and renewability, thus representing an interesting renewable feedstock. While chemical modification allows for precise tailoring of their properties, greater emphasis on sustainability aspects of such processes, for instance a reduction of the produced waste and avoidance of toxic substances, should be aimed for. This work thus focuses on a more sustainable and efficient two-step synthetic alternative approach for the alkylation of  $\beta$ -cyclodextrin ( $\beta$ -CD), especially avoiding the typical use of highly toxic alkylating agents. Transesterification using vinyl acetate facilitated a more sustainable acetylation of  $\beta$ -CD, resulting in an *E*-factor of 2.83 for the overall process. In a subsequent step, the acetylated  $\beta$ -CDs were successfully reduced under mild conditions to ethylated  $\beta$ -CDs (RE- $\beta$ -CDs) using near-stoichiometric amounts of TMSD and 4 mol%  $\text{GaBr}_3$  per ester group, whereby also new mechanistic insights were gained. Notably, anisole was introduced as a more benign, bioavailable alternative to the traditionally used hazardous solvents (e.g. dichloromethane, chloroform). Herein, we present the synthesized RE- $\beta$ -CDs, which exhibited properties comparable to methylated analogues, including solubility ( $\text{H}_2\text{O}$ , MeOH, EtOH, DMSO), thermal stability (TGA/DSC), and host-guest interactions, as confirmed by 2D DOSY and ROESY NMR spectroscopy. Overall, this study establishes a more environmentally friendly access to alkylated  $\beta$ -CDs without compromising characteristic properties of conventionally synthesized methylated CDs, offering a generally more sustainable alternative approach.

Received 16th July 2025  
Accepted 31st July 2025

DOI: 10.1039/d5su00590f

rsc.li/rscsus

## Sustainability spotlight

This work demonstrates a more sustainable alkylation strategy of  $\beta$ -cyclodextrin ( $\beta$ -CD), an interesting renewable oligosaccharide with various application possibilities, for instance in phase transfer catalysis or water purification. The focus was to establish a process that minimizes waste and avoids typically used hazardous substances, instead utilizing more benign and non-toxic compounds, closely following the principles of *Green Chemistry*. Significant recycling rates for solvents (acetonitrile 96%, isopropanol 94%), use of catalysts, and high conversions facilitated a low environmental impact, reaching an *E*-factor for the acetylation of 2.83. Additionally, hazardous solvents could successfully be substituted by non-toxic and bio-based alternatives.

## Introduction

Cyclodextrins (CDs) are an intriguing class of bio-based oligosaccharides, obtained by the enzymatic conversion of naturally occurring starch.<sup>1,2</sup> CDs form conically-shaped macrocycles, consisting of six, seven, or eight glucose units connected *via*  $\alpha$ -1,4-glycosidic bonds ( $\alpha$ -CD,  $\beta$ -CD, and  $\gamma$ -CD, respectively).<sup>3,4</sup>

Their low toxicity, renewability, and biodegradability are exemplary properties of native CDs, directly contributing to the principles of *Green Chemistry*.<sup>5,6</sup> In addition, their characteristic hydrophobic inner cavity, in contrast to the hydrophilic outer periphery, facilitates the formation of non-covalent inclusion complexes with various guest molecules, making their use especially attractive for drug delivery in pharmaceutical applications, catalysis, food sciences, cosmetics, or environmental engineering.<sup>7-12</sup> Although, chemical modification of the macrocycle provides the opportunity to further tailor the physicochemical properties to unique needs, the aspect of sustainability of the necessary chemical transformations is often neglected. Acetylated  $\beta$ -CD, one of the first reported classes of CD derivatives, is conventionally synthesized by the use of excessive amounts of acetic anhydride.<sup>13,14</sup> Strategies aiming at

<sup>a</sup>Institute of Biological and Chemical Systems – Functional Molecular Systems (IBCS-FMS), Karlsruhe Institute of Technology (KIT), Hermann-von-Helmholtz-Platz 1, 76344 Eggenstein-Leopoldshafen, Germany. E-mail: m.a.r.meier@kit.edu; Web: <https://www.meier-michael.com>

<sup>b</sup>Institute of Organic Chemistry (IOC), Karlsruhe Institute of Technology (KIT), Kaiserstraße 12, 76131 Karlsruhe, Germany

<sup>c</sup>Institut de Chimie de Strasbourg, Université de Strasbourg, UMR 7177 CNRS, 4 rue Blaise Pascal, CS90032, 67081 Strasbourg Cedex, France



improved sustainability have been explored by utilizing ionic liquids or vinyl acetate as “greener” solvent or reagent alternatives, respectively.<sup>15,16</sup> Vinyl acetate in particular displays a more favorable atom economy, lower toxicity, non-corrosiveness, and generally milder reaction conditions, compared to acetic anhydride.<sup>17,18</sup> Accordingly, Meier *et al.* demonstrated the use of vinyl acetate for the acetylation of cellulose, resulting in a reduced environmental impact, illustrated by significantly reduced *E*-factors and milder reaction conditions.<sup>19</sup> Among numerous different CD derivatives, alkylated CDs are of particular interest due to their unique physicochemical characteristics.<sup>20,21</sup> Methylation of CDs enhances water solubility, reduces crystallinity, and alters host-guest interactions with non-polar guest molecules by tuning the degree of substitution (DS) to value of desired properties.<sup>22–24</sup> The synthesis of CD ethers predominantly involves the use of highly toxic and carcinogenic alkylation reagents (methyl iodide, ethyl chloride, or dimethyl sulfate) in combination with hazardous solvents (*e.g.* *N,N*-dimethylformamide) under strong basic conditions (sodium hydride or sodium hydroxide).<sup>25–29</sup> These routes are associated with high environmental factors (*E*-factor) and significant safety concerns. The *E*-factor is a promising metric used for assessing the environmental impact of chemical processes. It is defined as the mass ratio of generated waste to desired product obtained, accounting for yields, reagents, side products, solvent losses, and auxiliary materials.<sup>30</sup> However, a relevant limitation of the *E*-factor is its neglect of toxicity aspects of the substances involved, an important factor that significantly influences both the sustainability and safety of a process, as emphasized by the general principles of *Green*

*Chemistry*.<sup>6,31</sup> Therefore, the focus of benign and more sustainable reagents should be emphasized in addition to minimizing waste production of chemical processes. The aim of this work is to present an alternative pathway towards alkylated CDs, while avoiding hazardous substrates and focusing on lowering the environmental impact. A comprehensive investigation in relation to sustainability aspects was conducted for a vinyl acetate-based acetylation of  $\beta$ -CD and the reaction parameters were optimized accordingly. Novel insights into a subsequent silane-based GaBr<sub>3</sub>-catalyzed ester reduction were furthermore gained and the established reaction parameters were evaluated in terms of sustainability compared to present methods.<sup>32–35</sup> Herein, we thus report a more sustainable synthesis of ethylated  $\beta$ -CDs with comparable host-guest and physicochemical properties to conventional methylated  $\beta$ -CDs.

## Results and discussion

### More sustainable synthesis and characterization of acetylated- $\beta$ -cyclodextrin

For a less toxic and non-carcinogenic access to etherified  $\beta$ -CD derivatives, a two-step strategy was developed: acetylation followed by deoxygenative reduction towards CD ethers. A more sustainable synthesis route for the acetylation of  $\beta$ -CD was thus first investigated. The acetylation of the cyclic oligomer was conducted utilizing vinyl acetate as an acetylating reagent, a generally more sustainable and less toxic alternative to the established acetic anhydride route for carbohydrate modification.<sup>19</sup> Due to the formation of vinyl alcohol as a side product, which tautomerizes to the thermodynamically favored

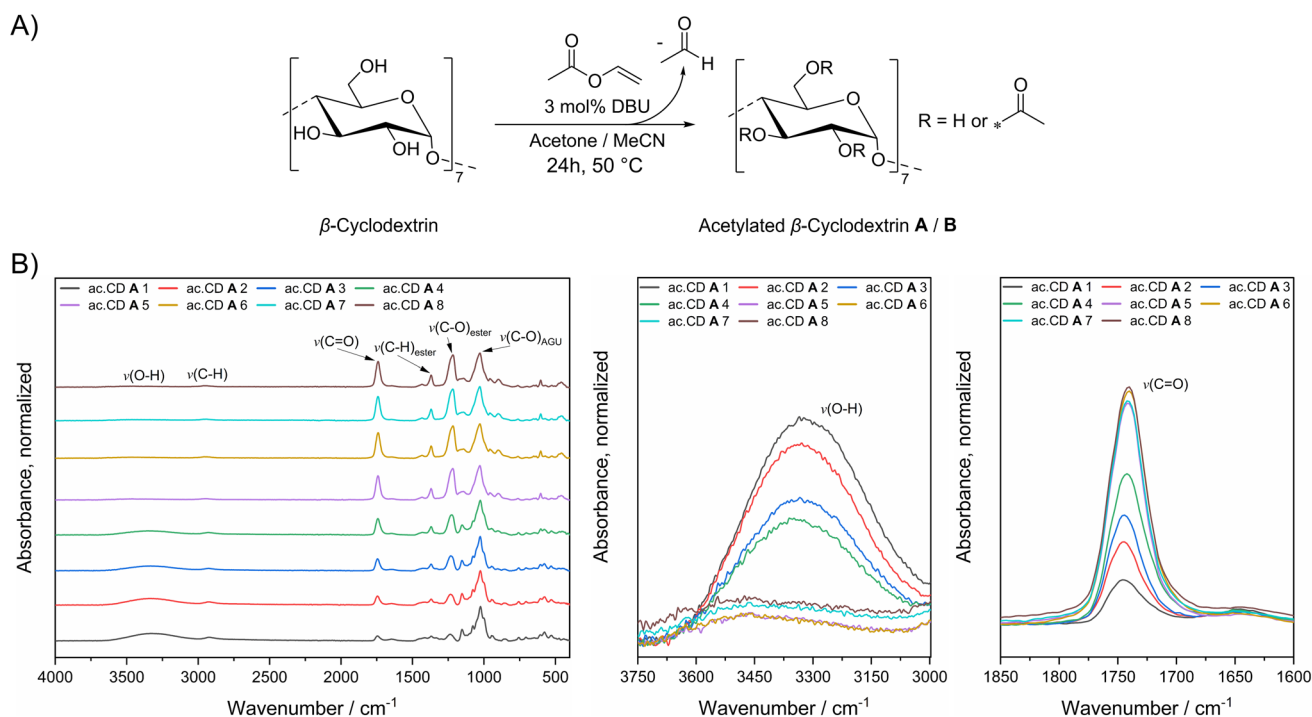


**Fig. 1** (A) General reaction scheme and conditions of the DBU-catalyzed acetylation of  $\beta$ -CD with vinyl acetate in acetone or acetonitrile. (B) ATR-IR spectra (left) of ac.CD A 1–8 and the detailed comparison of the O–H stretching vibration (middle) and C=O stretching vibration (right).



**Table 1** Synthesized acetylated  $\beta$ -CD samples per used equivalents of vinyl acetate (VA) in acetone (A) or acetonitrile (B) and the corresponding conversions, yields, and calculated DS (degree of substitution,  $DS_{\max} = 21.0$  for  $\beta$ -CD) based on  $^1\text{H}$  NMR (SI, eqn (1)) and  $^{31}\text{P}$  NMR (SI eqn (2) and (3)) spectroscopy methods

Sample	Equiv. VA	Conversion <sup>a</sup> /%	Yield <sup>a</sup> /%	$DS_{1\text{H}}$	$DS_{31\text{P}}$
ac.CD A 1	6.00	40	64	1.47	2.38
ac.CD A 2	9.00	44	59	2.17	4.00
ac.CD A 3	12.0	47	66	4.27	5.67
ac.CD A 4	15.0	63	71	7.49	9.38
ac.CD A 5	18.0	99	67	16.9	17.8
ac.CD A 6	21.0	87	74	17.8	18.3
ac.CD A 7	24.0	76	65	17.5	18.2
ac.CD A 8	27.0	71	72	18.3	19.0
ac.CD B 1	6.00	48	68	1.68	2.87
ac.CD B 2	9.00	72	61	4.13	6.51
ac.CD B 3	12.0	96	63	11.0	11.6
ac.CD B 4	15.0	93	61	12.8	14.0
ac.CD B 5	18.0	Quant. <sup>b</sup>	82	18.0	18.3
ac.CD B 6	21.0	95	89	20.0	20.0
ac.CD B 7	24.0	85	72	20.2	20.4
ac.CD B 8	27.0	74	77	20.0	20.0

<sup>a</sup> Determined based on the  $DS_{31\text{P}}$ . <sup>b</sup> Assumption of quantitative conversion due to calculated conversion of 102% (within expected NMR error).

acetaldehyde (b.p. 20 °C), the chemical equilibrium shifts at elevated temperatures, driving the acetylation of  $\beta$ -CD and thus minimizing the amount of required modification reagent. Therefore, the transesterification was performed at 50 °C, facilitating efficient conversions while preventing vinyl acetate (b.p. 72 °C) from evaporating from the reaction mixture. In addition, vinyl acetate displays the advantage, in comparison to acetic anhydride, that the formed side product (acetaldehyde) does not interfere with the use of common organic bases, e.g. 1,8-diazabicyclo[5.4.0]undec-7-ene (DBU), by the formation of the corresponding salt.<sup>36</sup> This simplifies the subsequent

recycling process and further enables base catalysis, which aligns with the general principles of *Green Chemistry*. Thus, 3 mol% DBU per AGU were added to pre-dried  $\beta$ -CD and vinyl acetate to catalyze the transesterification reaction. The aforementioned substrates were suspended in either acetone or acetonitrile, both regarded as greener aprotic solvent alternatives compared to the typically applied DMF (Fig. 1A).<sup>37</sup> After 24 h of stirring, the acetylated  $\beta$ -CDs were purified by refluxing in isopropanol, avoiding undesired side reactions observed with more nucleophilic alcohols such as methanol or ethanol in the presence of DBU, which would result in lower yields, undesired side products, and increased total waste as reported by Meier and co-workers.<sup>19</sup> In order to optimize and evaluate the reaction, a set of acetylated  $\beta$ -CDs (ac.CD A/B 1–8) was synthesized by using various stoichiometric ratios (6.00–27.0 equiv.) of vinyl acetate in acetone (A) or acetonitrile (B) (Table 1).

ATR-IR spectroscopy was used to monitor the general trend of conversion by analyzing the signal intensities of the O–H stretching vibration at 3305  $\text{cm}^{-1}$ , the C=O stretching vibration at 1742  $\text{cm}^{-1}$ , the C–H stretching vibration corresponding to the ester at 1368  $\text{cm}^{-1}$ , and the C–O stretching vibration at 1236  $\text{cm}^{-1}$  of the formed ester moiety (Fig. 1B left). To allow comparability between the different ATR-IR data, spectra were normalized to the vibrational band at 1022  $\text{cm}^{-1}$ , which corresponds to the invariant C–O–C acetal bond of the AGU.

With increasing equivalents of vinyl acetate, an increasing carbonyl vibrational band, suggesting successful and increased conversion to the acetylated  $\beta$ -CD, can be detected (Fig. 1B right). The conversions of the samples ac.CD A 5–8 were significantly higher than the others, which is consistent with the decreasing signal intensities of the O–H stretching vibration (Fig. 1B middle). An equivalent trend is visible for the transesterification in acetonitrile (SI, Fig. S50). The yield of the reactions was generally acceptable and good for higher conversions, but correlated poorly with the conversions, most likely due to significant solubility differences of the modified CDs with different DS. To evaluate the efficiency of the transesterification, the degree of substitution (DS

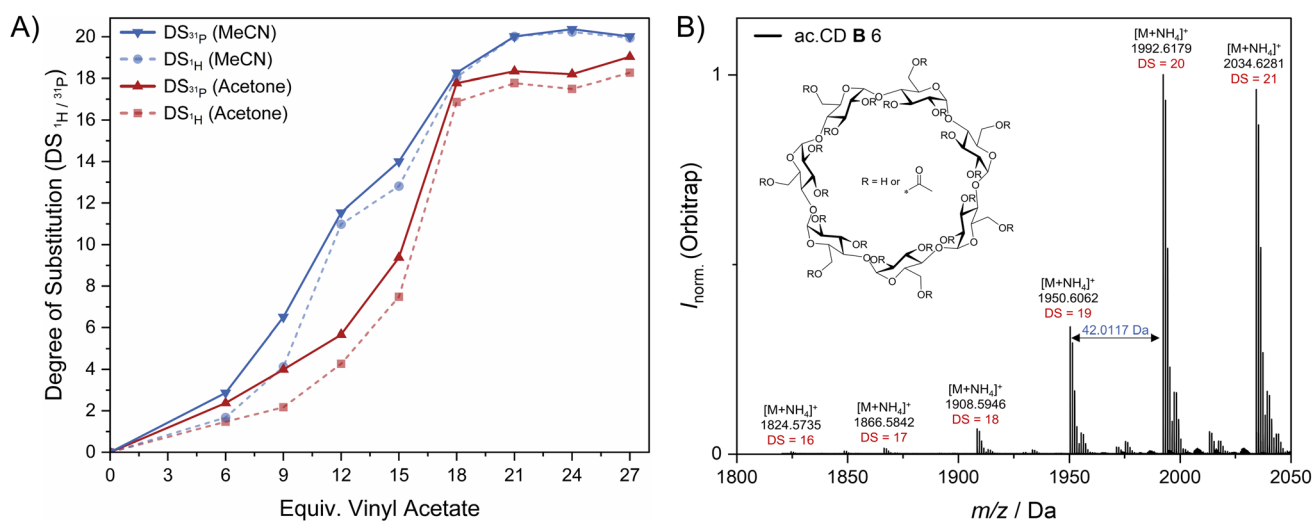


**Fig. 2** (A) Calculated DS based on  $^{31}\text{P}$  NMR (solid) or  $^1\text{H}$  NMR (dashed) in relation to the applied equivalents of vinyl acetate in acetone (red) and acetonitrile (blue). (B) ESI-MS spectrum for the illustration of the DS distribution of sample ac.CD B 6 ( $DS_{31\text{P}} = 20.0$ ).



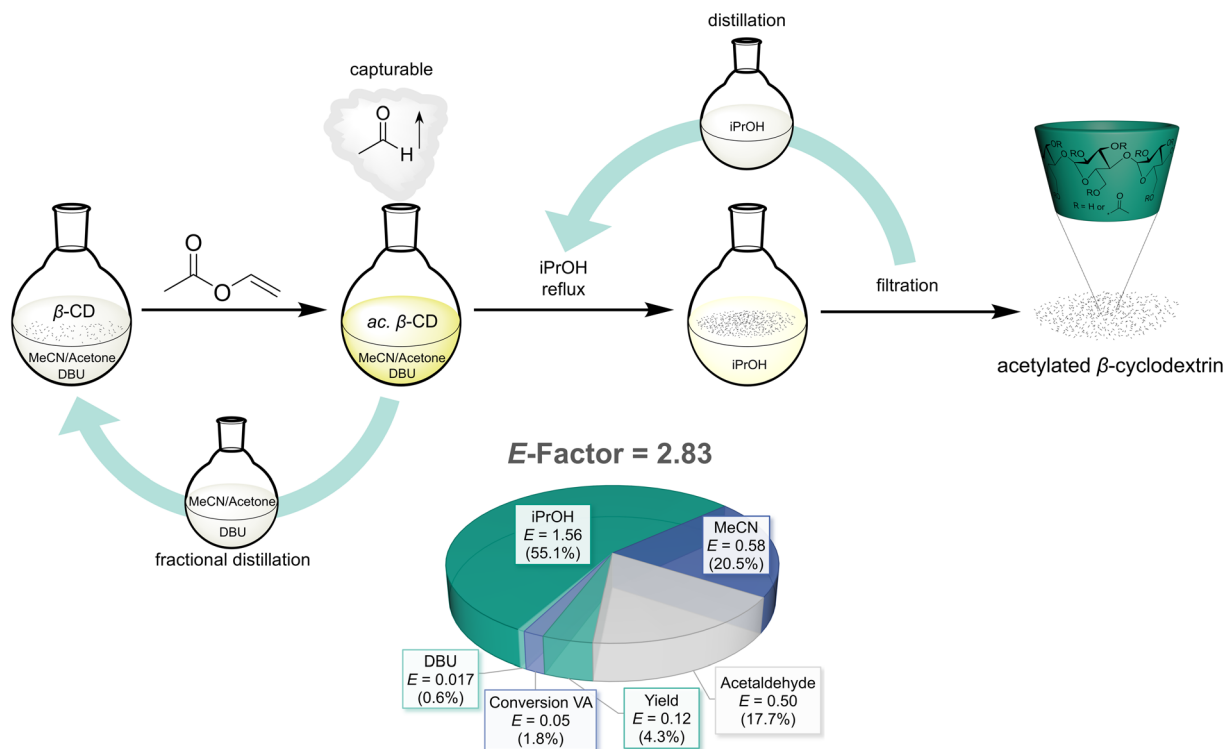


Fig. 3 A schematic illustration of the  $\beta$ -CD acetylation recycling approach. Pie chart of the calculated  $E$ -factor (SI, eqn (4)) for the synthesis of ac.CD **B 6** with the respective contribution of the utilized substrates, formed products, recovered solvents, and yield loss.

where  $DS_{\max} = 21.0$  for  $\beta$ -CD) of ac.CD **A/B 1–8** was thoroughly investigated *via* previously reported  $^1\text{H}$ - and  $^{31}\text{P}$ -NMR spectroscopy methods (SI, Fig. S1–S16).<sup>38</sup>

Accordingly, Fig. 2A displays the calculated DS based on  $^1\text{H}$  NMR (dashed) and  $^{31}\text{P}$  NMR (solid) spectroscopy, which agree well with each other, in the two solvent systems. In both solvents, the proposed synthesis strategy gives access to a broad spectrum of various  $DS_{31\text{P}}$  in the range of 2.38 to 20.4 for acetylated  $\beta$ -CDs (detailed in Table 1). These results suggest a general trend for higher conversions by performing the transesterification in acetonitrile rather than acetone. Only by using acetonitrile, CD derivatives close to peracetylation ( $DS = 20.4$ ) could be obtained. On the other hand, samples of lower DS ( $\leq 19.0$ ) have also been synthesized using the less toxic and more environmentally friendly solvent, acetone. In addition to NMR studies, electrospray ionization mass spectrometry (ESI-MS) was utilized to gain further insights into the structural composition of the synthesized samples (Fig. 2B). The individual acetylated  $\beta$ -CD species of a distinct DS (Fig. 2B marked in red) and the characteristic shift of 42.011 Dalton (Da) (Fig. 2B marked in blue) illustrate the general distribution of various DS along the sample ac.CD **B 6**. Besides the structural characterization, the synthesized samples ac.CD **A/B 1–8** were also investigated in relation to their thermal properties *via* differential scanning calorimetry (DSC). The DSC measurements indicated no melting point ( $T_m$ ), but identified glass transition temperatures ( $T_g$ ) for all acetylated  $\beta$ -CD samples (except ac.CD **A 1**), revealing an amorphous state in the measured temperature range, as can be expected for a mixture of compounds

(confirm Fig. 2B). Increasing functionalization of the hydroxyl groups led to the loss of hydrogen bond donors, thereby diminishing the inter- and intramolecular hydrogen bond network. As a result, the  $T_g$  is steadily decreasing from 236.2 °C ( $DS_{31\text{P}} = 2.87$ ) to 129.0 °C ( $DS_{31\text{P}} = 20.4$ ) with increasing DS (SI, Fig. S57 and S58). To evaluate the proposed acetylation procedure in terms of sustainability, a comprehensive solvent recycling approach was designed (Fig. 3). As a result of the optimized reaction conditions, in relation to conversion and yield (Table 1), and the evaporation of acetaldehyde, the only side product, from the reaction mixture, the utilized solvents during the reaction and purification steps display a crucial role in the total contribution to the  $E$ -factor. Simple distillation methods facilitated recycling rates up to 96% for acetonitrile and 94% for isopropanol (exact values in SI, Table S2), leading to an  $E$ -factor of 2.83 (Fig. 3) for ac.CD **B 6**. The employed solvents have been regained in high purity ( $^1\text{H}$  NMR spectra in SI, Fig. S59 and S60) and could be reused in a consecutive reaction. Due to the use of minimal catalytic amounts of DBU, its recycling was not further pursued, but could very well be realized on a larger scale.<sup>19</sup> Similarly, acetaldehyde (b.p. 20 °C) can theoretically be captured by fractionating columns, contributing a valuable bulk chemical.

#### Synthesis of randomly ethylated $\beta$ -CD (RE- $\beta$ -CD) *via* $\text{GaBr}_3$ -catalyzed reduction of acetylated $\beta$ -CD with 1,1,3,3-tetramethyldisiloxane (TMDS)

In a subsequent reaction step, the acetylated  $\beta$ -CD samples were reduced applying a TMDS-mediated  $\text{GaBr}_3$ -catalyzed reduction



to obtain RE- $\beta$ -CD. The bifunctional organosilane TMDS can be considered as a side product of the silicone industry, making its utilization as a reducing reagent valuable.<sup>39</sup> GaBr<sub>3</sub> was used in catalytic amounts to facilitate the conversion from the ester to the corresponding ether, while maintaining mild reaction conditions. This type of reaction typically proceeds in carcinogenic and hazardous solvents, e.g. dichloromethane, chloroform, or benzene.<sup>33,40</sup> In perspective to sustainability, the replacement towards a non-toxic alternative is highly desirable. Therefore, we report the use of anisole as a comparatively non-toxic, non-carcinogenic, non-volatile, and bio-available substitute to reduce acetylated  $\beta$ -CD to RE- $\beta$ -CD at mild conditions (Fig. 4A).<sup>41,42</sup> In order to optimize the reaction conditions and minimize the amount of produced waste, the reaction was monitored *via* ATR-IR spectroscopy. Similarly to the optimization of the acetylation reaction, the intensity of the C=O stretching vibrational band at 1739 cm<sup>-1</sup> was investigated for various reaction conditions (Fig. 4B).

First, the conversion was investigated as a function of reaction time, applying reaction conditions comparable to literature reports (2 mol% GaBr<sub>3</sub> and 1.10 equiv. TMDS per ester).<sup>34,35</sup> As illustrated by the corresponding ATR-IR spectrum (Fig. 4B left), reduction of the ester was achieved using these parameters as indicated by the decreasing C=O vibrational band, but even after 161 hours full conversion was not achieved. Thus, the

influence of the catalyst and the reducing reagent was assessed. Increases in TMDS and GaBr<sub>3</sub> dosage both displayed a positive influence on the reaction rates and conversion (Fig. 4B middle and right), whereby the catalyst loading showed a more pronounced effect. Increasing the amount of catalyst is preferred here from a sustainability standpoint due to the potential recyclability and the overall much lower amounts. Indeed, the absolute quantity of substance would be significantly enhanced by increasing the stoichiometric amount of TMDS, resulting in more total waste. Concluding, 4 mol% GaBr<sub>3</sub> and 1.10 equivalents TMDS per ester moiety proved to be the preferred reaction parameters, assuring close to quantitative conversion and good yield (80%), contributing to minimizing the environmental impact. To quench the reaction, deionized water was added to the mixture in order to hydrolyze the reactive species and the combined solvents were removed *via* distillation. The residue was dissolved in ethanol and the hydrolyzed gallium salts were filtered off over Celite®. Afterwards, the solution was precipitated in *n*-hexane to dissolve *in situ* generated oligo- and polydimethylsiloxanes. Inductively coupled plasma optical emission spectrometry (ICP-OES) confirmed that the removal of gallium exceeded 99%, whereas no silicon traces were detected in the final product. In addition, the investigation of the structural properties of the RE- $\beta$ -CD was conducted *via* NMR spectroscopy. The conversion of the

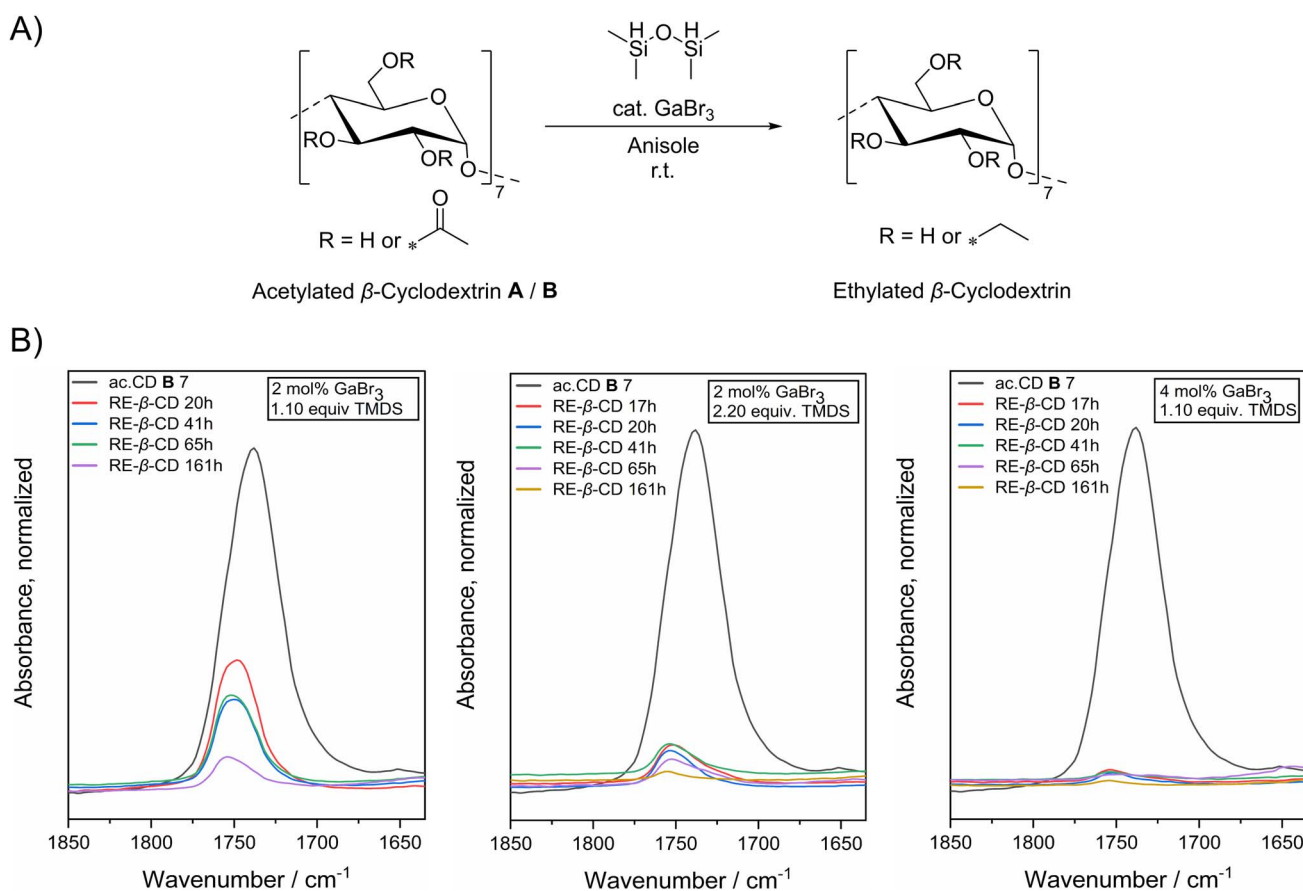


Fig. 4 (A) Reaction scheme of the GaBr<sub>3</sub>-catalyzed reduction of acetylated  $\beta$ -CD with 1,1,3,3-tetramethyldisiloxane (TMDS) in anisole. (B) ATR-IR monitoring of the C=O stretching vibration for different reaction conditions (as shown in the top right corner of the respective spectrum).



reduction was determined as 97% *via*  $^1\text{H}$  NMR by comparing the values of the integrals corresponding to the methyl groups of the acetyl and ethyl moieties (SI, Fig. S51). In addition, the RE- $\beta$ -CD equivalent of ac.CD **B 7** was derivatized with TMDP and quantitative  $^{31}\text{P}$  NMR spectroscopy, analogously to the before-mentioned DS determination, was performed. The results demonstrate that a substantial overreduction, *i.e.* the cleavage of the ethyl ether moieties, occurred, leading to unmodified hydroxyl groups (SI, Fig. S17). The final DS of the RE- $\beta$ -CD sample was calculated to be  $\text{DS}_{31\text{P}} = 14.3$ , the DS distribution revealed by mass spectrometry further confirms these findings (SI, Fig. S54). Additionally, the  $^{13}\text{C}$  NMR spectrum indicated the successful conversion by the absence of the carbonyl carbon specific signal and the expected downfield shift of the C6 carbon to 68.42 ppm (SI, Fig. S52). Nevertheless, an additional signal at 60.12 ppm was detected, which usually correlates to the respective unmodified C6-OH carbon. Thus, the cleavage of the ether preferably occurs at the C6 position, which is advantageous from a synthetic point of view due to easier further modification.

The intriguing characteristics of CD derivatives predominantly arise from their cyclic and conical shape. Besides spectroscopic studies, size exclusion chromatography (SEC) was selected to investigate the stability of this macrocyclic structure during the acetylation and reduction reaction. Cleavage products of lower molecular weight would be indicated by signals of higher retention times in the SEC traces. Exemplarily, the SEC traces of ac.CD **B 7** and RE- $\beta$ -CD display no further signals of higher retention times, relative to the respective main product peak, indicating no cleavage products and consequently the stability of the macrocyclic structure during the derivatization steps. In comparison to unmodified  $\beta$ -CD, the SEC trace of the main product peak of RE- $\beta$ -CD shifts towards higher retention times. This phenomenon was also observed by the even higher

shift of the main product peak of permethylated  $\beta$ -CD (PM- $\beta$ -CD). With the progressive functionalization of the hydroxyl groups (for PM- $\beta$ -CD full conversion), the hydrogen bond network, contributing to the general rigidity of the conical structure, is lost. As a consequence, a more flexible geometry can be obtained, reducing the hydrodynamic radius and therefore resulting in higher retention times. Surprisingly, the SEC trace of RE- $\beta$ -CD shows low intensity signals at lower retention times than the main product peak, indicating the formation of species of higher molecular weight during the reduction (Fig. 5A). In contrast, the mass spectrum of RE- $\beta$ -CD only displays the expected signals for ethylated cyclodextrins of varying DS. However, no signals could be assigned to any compound that would explain the emergence of the higher molecular weight peaks in the SEC trace (SI, Fig. S54). Thus, to gain further understanding related to this SEC peak, a model reduction with a less complex substrate was conducted. Glycerol triacetate (triacetin) was selected as the model substrate due to its easy accessibility and nature as a polyfunctional acetate ester of low molecular weight. Triacetin was subjected to the optimized reduction conditions (Fig. 4B right) and crude ESI-MS analysis was conducted (Fig. 5B). The mass spectrum shows the presence of the expected reduction product triethylin (molecule (1) in Fig. 5B) and residual triacetin (molecule (2) in Fig. 5B). However, signals at higher  $m/z$  values are visible as well. The mass peak at  $m/z = 373.2558$  Da corresponds exactly to a product dimer, *i.e.* the mass of two molecules of triethylin minus two hydrogen atoms (molecule (4) as a representative structure in Fig. 5B). Furthermore, the signal at  $m/z = 345.2246$  Da can be assigned to the same molecule with one ethoxy group replaced by a hydroxy group (molecule (3) in Fig. 5B), resulting from the beforementioned overreduction of molecule (4). The presence of these signals serves as a strong indication that a previously unreported intermolecular coupling

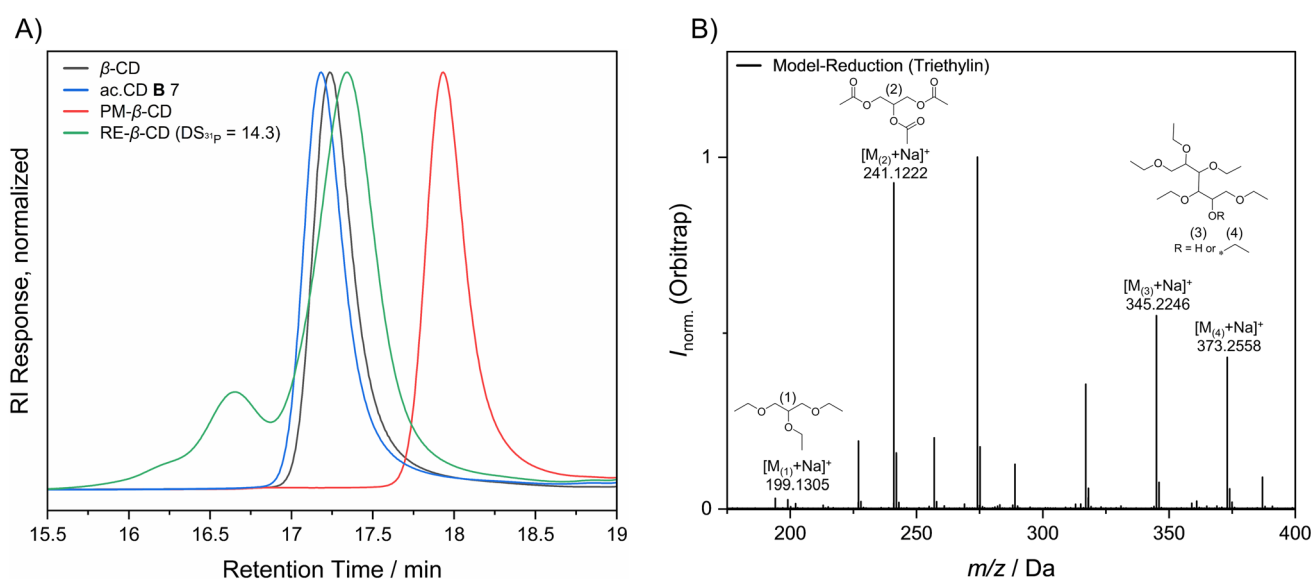


Fig. 5 (A) SEC traces of  $\beta$ -CD, ac.CD **B 7**, PM- $\beta$ -CD, and RE- $\beta$ -CD conducted in DMAc (0.034 wt% LiBr). (B) ESI-MS spectrum of the model reduction of triacetin (2) to triethylin (1) depicting possible structures (isomers thereof are likely) of the formed coupling products (3) and (4) as sodium adducts.



occurs as a side reaction during the GaBr<sub>3</sub>-catalyzed reduction. Such a side reaction is in agreement with the mechanism suggested by Sakai *et al.* for silane-mediated ester reductions, involving radical intermediates that can recombine to form the respective coupled species (SI, Scheme S1).<sup>43</sup> This postulate was based on the inhibition of the reduction in the presence of radical scavengers, as well as poor yields for substrates with radical-stabilizing substituents, such as aromatic esters. We propose that radical–radical recombination could serve as a possible pathway for the formation of the higher molecular weight products observed in the ESI-MS spectrum (Fig. 5B). Although not detectable in the mass spectrum of RE-β-CD, we assume that this side reaction is also responsible for the emergence of the additional signals in the corresponding SEC trace. These observations are in line with the proposed radical reaction mechanism and thus further supports this mechanism.<sup>43</sup> Similar to the acetylation procedure, a sustainability assessment was conducted for this reaction. To evaluate its environmental impact, attempts were made to recycle the used solvents (anisole, water). However, effective separation of the solvent mixture could not be achieved yet with available equipment and due to small scales. Thus, a simplified environmental factor ( $E_{\text{simple}}$ -factor), which excludes the contribution of the solvents, was employed as a metric to quantify waste generation. The  $E_{\text{simple}}$ -factor was calculated to be 4.22.

### Investigation of the host–guest and physicochemical properties of RE-β-CD

In order to investigate the ability of the synthesized RE-β-CD to form inclusion complexes, 2D NMR diffusion ordered

spectroscopy (DOSY) and rotating frame Overhauser enhancement spectroscopy (ROESY) studies were conducted. In both cases, anisole (a suitable non-polar guest molecule) and RE-β-CD (host molecule) were combined in a 1 : 1 molar ratio in deuterated water. The formation of an inclusion complex was first examined *via* DOSY NMR. The free anisole and RE-β-CD molecules display distinctly different hydrodynamic radii, which correlate to varying diffusion coefficients ( $D$ ) stated by the Stokes–Einstein equation. However, in the DOSY NMR spectrum, only one value of  $D = 2.86 \times 10^{-6} \text{ cm}^2 \text{ s}^{-1}$  was obtained (Fig. 6A), indicating both molecules diffuse together as a single entity. This value is significantly lower to the theoretical diffusion coefficient of anisole in water,  $D_{\text{theo.}} = 7.01 \times 10^{-6} \text{ cm}^2 \text{ s}^{-1}$ , and aligns with literature reports of comparable systems (SI, eqn (7)), thus implying that an incorporation into the CD cavity took place and an inclusion complex was formed (representative illustration of the inclusion complex in Fig. 6A).<sup>44</sup> To gain further insight into the structural composition of the host–guest complex, ROESY studies have been performed. The data reveal an intermolecular H–H cross coupling between the aromatic anisole protons at 7.40–7.02 ppm and the inner cavity protons of RE-β-CD (H<sub>3</sub> at 3.60 ppm, H<sub>5</sub> at 3.75 ppm), schematically illustrated by the dotted lines in Fig. 6B. This spatial proximity is direct evidence of the incorporation of anisole (guest) into the RE-β-CD's cavity (host).

In addition to the detailed structural analysis, the physicochemical properties, which ultimately dictate the processibility and general field of application, were studied. Solubility tests revealed that polar solvents, *e.g.* H<sub>2</sub>O, MeOH, and EtOH, are suitable candidates for the dissolution of RE-β-CD.

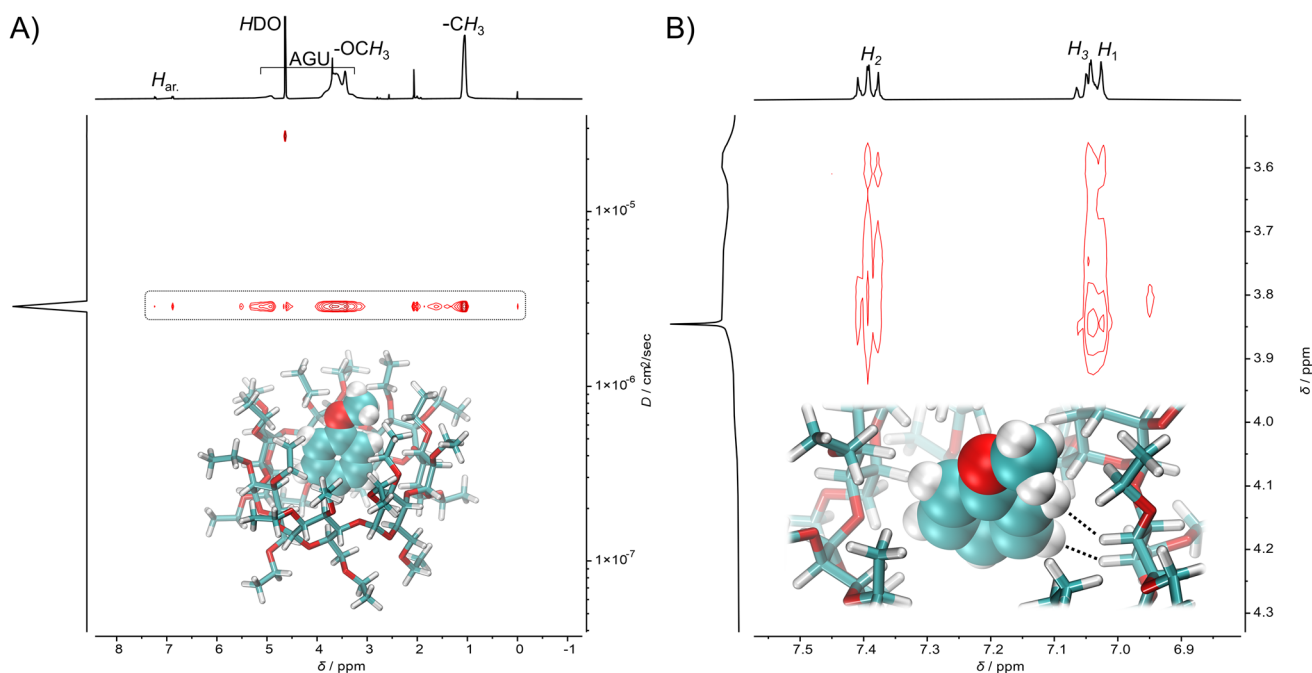


Fig. 6 Investigation of the formation of host–guest interactions between RE-β-CD and anisole *via* (A) 2D DOSY and (B) 2D ROESY experiment for the illustration of the intermolecular H–H correlation between RE-β-CD and anisole, indicated by the dotted lines. Both 2D NMR experiments were conducted in D<sub>2</sub>O at a 1 : 1 molar ratio. For the 3D illustrations, the host–guest inclusion complex was adapted from a crystal structure,<sup>45</sup> partially optimized at the B3LYP-D3/6-31G(d,p) level of theory using Gaussian 16.<sup>46</sup>



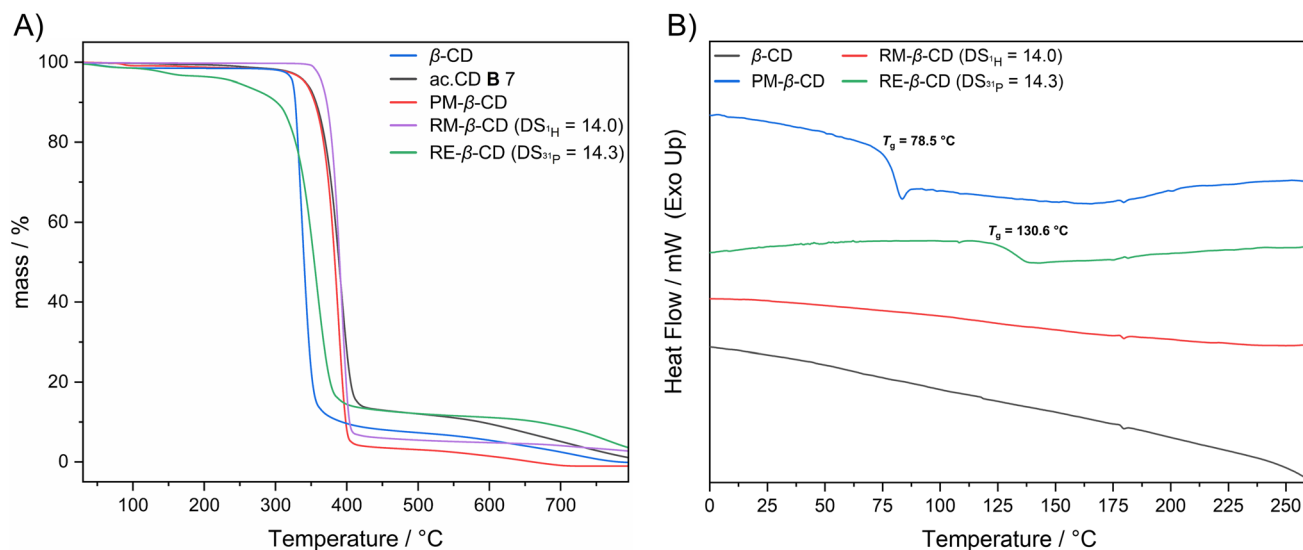


Fig. 7 (A) TGA decomposition curves of  $\beta$ -CD, ac.CD **B 7**, PM- $\beta$ -CD, RM- $\beta$ -CD, and RE- $\beta$ -CD in the range of 25 °C to 800 °C. (B) DSC studies (second heating cycle) of  $\beta$ -CD, PM- $\beta$ -CD, RM- $\beta$ -CD, and RE- $\beta$ -CD in the range of 0 °C to 275 °C and depiction of the respective  $T_g$  values.

Additionally, aprotic alternatives, *i.e.* DMSO, DMAc, and DMF, efficiently dissolve RE- $\beta$ -CD as well. Thermogravimetric analysis (TGA) measurements were conducted in the range of 25 °C to 800 °C to compare and determine thermal stability of the synthesized RE- $\beta$ -CD and ac.CD **B 7** (exemplarily for acetylated  $\beta$ -CDs) samples (Fig. 7A). The TGA traces reveal a single-step degradation for the investigated samples in the range of 300 °C to 420 °C, attributed to the decomposition of the CD backbone. The thermal decomposition values ( $T_d$ ) of the derivatized CDs indicate an improved thermal stability compared to native  $\beta$ -CD, whereas RE- $\beta$ -CD showed the lowest  $T_{d50\%} = 354.4$  °C of the CD derivates (exact  $T_{d5\%}$  and  $T_{d50\%}$  values in SI, Table S1). Due to residual physically bound water,  $T_{d5\%}$  values of RE- $\beta$ -CD cannot be qualitatively compared to the remaining samples. To complement the TGA analysis, DSC measurements were conducted. While no thermal transition could be detected for randomly methylated  $\beta$ -CD (RM- $\beta$ -CD) ( $DS_{1H} = 14.0$ ), the DSC analysis of RE- $\beta$ -CD reveals an amorphous state in the investigated temperature region (0–275 °C) by showing a glass transition at 130.6 °C (Fig. 7B). Although the DS values are comparable, these results cannot only be attributed to the difference in the side chain substituent, due to potentially different substitution patterns resulting from the aforementioned ether cleavage.

## Conclusion

This work demonstrated a more sustainable and efficient two-step synthetic alternative strategy for ethylated  $\beta$ -CD, avoiding typically used highly toxic alkylation agents. The first step involved a previously reported protocol for vinyl acetate-based transesterification, which achieved a “greener” acetylation pathway with a notably low *E*-factor of 2.83 through catalytic dosage of DBU and high recycling rates for the employed solvents, acetonitrile (96%) and isopropanol (94%). In the

second step, the acetylated  $\beta$ -CDs were efficiently reduced to RE- $\beta$ -CDs under mild conditions, reaching high conversions by employing close to stoichiometric amount of TMDS and 4 mol% GaBr<sub>3</sub> per ester group. Herein, we reported the novel use of anisole, a non-toxic, bio-available solvent alternative to its conventional hazardous and carcinogenic counterparts. These carefully optimized parameters, monitored by ATR-IR spectroscopy, ensured efficient reaction progress while minimizing waste generation. Through a model reaction with triacetin, SEC analysis and mass spectrometry confirmed the existence of a previously unreported side reaction of the applied ester reduction, resulting in the formation of higher molecular weight side products, potentially arising from radical-radical recombination, thus offering new experimental insights into the mechanistic pathway of the GaBr<sub>3</sub>-catalyzed silane-based carbonyl-reduction reactions. The synthesized RE- $\beta$ -CDs exhibited physicochemical properties comparable to methylated CDs, including solubility in both protic (H<sub>2</sub>O, MeOH, or EtOH) and aprotic solvents (DMSO) and thermal stability as characterized by TGA and DSC analyses. Additionally, their host-guest properties with the non-polar guest molecule anisole was characterized through DOSY and ROESY NMR methods, to verify the formation of inclusion complexes. In conclusion, this work showcased a more benign synthetic alternative for etherification of  $\beta$ -CD. We have demonstrated that RE- $\beta$ -CDs obtained *via* the developed approach retain their characteristic performance without compromise, offering a more sustainable alternative to the conventionally synthesized  $\beta$ -CD derivatives.

## Experimental section

### Materials

Acetone (Thermo Scientific, extra dry 99.8%), acetonitrile (MeCN, Sigma-Aldrich, anhydrous 99.8%), acetylchlorid (Sigma-



Aldrich, 99%), anisole (Sigma-Aldrich, 99%), chloroform- $d_1$  ( $\text{CDCl}_3$ , Eurisotop, 99.80%),  $\beta$ -cyclodextrin ( $\beta$ -CD, Acros Chemicals, 98%), deuterium oxide ( $\text{D}_2\text{O}$ , Eurisotop, 99.90%),  $N,N$ -dimethyl acetamide (DMAc, Sigma, anhydrous 99.8%), dimethylsulfoxide- $d_6$  ( $\text{DMSO-}d_6$ , Eurisotop, 99.80%), 1,8-diazabicyclo[5.4.0]undec-7-ene (DBU, Tokyo Chemical Industry, <98%), gallium bromide ( $\text{GaBr}_3$ , Thermo Scientific Chemicals, ultra dry 99.998%), glycerol (abcr, 99%) *endo-N*-hydroxy-5-norbornene-2,3-dicarboximide (*e*-HNDI, Alfa Aesar, 97%), lithium bromide ( $\text{LiBr}$ , Acros Organics, 99+%), pyridine (Thermo Scientific Chemicals, extra pure 99%), sodium carbonate ( $\text{Na}_2\text{CO}_3$ , Thermo Scientific, extra pure anhydrous 99.5%), sodium sulfate ( $\text{Na}_2\text{SO}_4$ , Thermo Scientific, extra pure anhydrous 99%), tetramethyldisiloxane (TMDS, Acros Chemicals, 97%), trifluoroacetic acid (TFA, Acros chemicals, extra pure 99%), and vinyl acetate (VA, Acros Chemicals, 99+) were used without further purification. Anisole was dried prior use by the addition of activated 4 Å molecular sieves. Only deionized water was used. Other solvents used are HPLC or analytical grade.

### General procedure for the synthesis of acetylation of $\beta$ -cyclodextrin

In a round bottom flask,  $\beta$ -cyclodextrin (300 mg, 0.264 mmol, 1.00 equiv.) was suspended in 7.5 mL anhydrous acetone or acetonitrile, followed by the addition of DBU (8.29  $\mu\text{L}$ , 0.0556 mmol, 1 mol% per -OH group). In addition, the respective amount of vinyl acetate (6.00–27.0 equiv.) was added dropwise under argon atmosphere. The heterogeneous solution was then heated to 50 °C and stirred for 24 h. The solvent mixture was removed under reduced pressure and the obtained precipitate was refluxed in 3 mL isopropanol. The mixture was cooled to -19 °C, isolated by vacuum filtration, and washed with cold isopropanol (3  $\times$  5 mL). Afterwards, the solid was dried at reduced pressure (10 mbar) at 65 °C for 24 h. The final product was obtained as a white powdery substance. Yields were calculated based on the  $\text{DS}_{31\text{P}}$  (Table 1) according to SI eqn (5) and (6).

### Reduction of acetyl- $\beta$ -cyclodextrin towards randomly ethylated $\beta$ -cyclodextrin (RE- $\beta$ -CD)

In a round bottom flask, acetylated  $\beta$ -cyclodextrin ( $\text{DS} = 20.1$ ) (5.00 g, 2.53 mmol, 1.00 equiv.) was dissolved in 125 mL anhydrous anisole.  $\text{GaBr}_3$  (629 mg, 2.03 mmol, 4 mol% per ester) dissolved in 5 mL anhydrous anisole was combined with the acetylated  $\beta$ -cyclodextrin solution. The homogeneous reaction mixture was stirred and TMDS (9.87 mL, 7.50 g, 55.9 mmol, 1.10 equiv. per ester) was added over the course of 3 h with a syringe pump. After 161 h, the mixture was quenched with water (50 mL) and the solvents (anisole/water) were removed under reduced pressure. The residue was dissolved in ethanol (50 mL), filtered over Celite® to remove any residual gallium species, and concentrated under reduced pressure. Afterwards, the mixture was precipitated from ethanol into cold *n*-hexane, vacuum filtered, and dried under vacuum (10 mbar) at 65 °C. The final product was obtained as a white powdery solid with

a yield of 80% (3.11 g, 2.03 mmol) (calculated based on the  $\text{DS}_{31\text{P}}$  according to SI eqn (5) and (6)).

ATR-IR:  $\nu/\text{cm}^{-1} = 3616\text{--}3161$   $\nu(\text{O-H})$ , 3007–2795  $\nu(\text{C-H})$ , 1084  $\nu(\text{C-O})_{\text{ether}}$ , 1030  $\nu(\text{C-O})_{\text{AGU}}$ .  $^1\text{H NMR}$  (400 MHz,  $\text{D}_2\text{O}$ ):  $\delta/\text{ppm} = 5.79\text{--}2.98$  (m, AGU, 7H), 3.84 (br,  $\text{CH}_2$ , 6H), 1.23 (t,  $J = 10.7$  Hz,  $\text{CH}_3$ , 9H).  $^{13}\text{C NMR}$  (126 MHz,  $\text{D}_2\text{O}$ ):  $\delta/\text{ppm} = 101.47$ , 80.69, 79.37, 71.70, 68.43, 66.86, 14.58, 14.14.

### Analytic methods

**Infrared spectroscopy (IR).** IR measurements were conducted, using a Bruker Alpha-p spectrometer (Ettlingen, Baden-Württemberg, Germany) with ATR technology in a range of  $\nu = 400\text{--}4000$   $\text{cm}^{-1}$ . Each measurement consisted of one background measurement and one absorbance measurement with 24 scans at room temperature.

**Nuclear magnetic resonance spectroscopy (NMR).** NMR spectroscopy was performed using a Bruker Ascend spectrometer (Ettlingen, Baden-Württemberg, Germany) (400 MHz for  $^1\text{H NMR}$ ) or Bruker Avance DRX (Ettlingen, Baden-Württemberg, Germany) (126 MHz for  $^{13}\text{C}$ , and 162 MHz for  $^{31}\text{P NMR}$ ) at a constant temperature of 298 K. For sample preparation, 5–25 mg of the samples were dissolved in deuterated solvents and mixed until homogeneous.  $^1\text{H NMR}$  spectra were recorded at 400 MHz with 16–64 scans (delay time  $d_1 = 1.00$  s),  $^{13}\text{C NMR}$  spectra were recorded at 126 MHz with 1024–16 384 scans (delay time  $d_1 = 1.00$  s), and  $^{31}\text{P NMR}$  spectra were recorded at 162 MHz with 512 scans (delay time  $d_1 = 5.00$  s). The chemical shifts ( $\delta$ ) were reported in parts per million (ppm) relative to the chemical shift of tetramethylsilane ( $\delta = 0.00$  ppm) and referenced to the solvent signal of  $^1\text{H}$ :  $\text{DMSO-}d_5$  at 2.50 ppm,  $\text{CHCl}_3$  at 7.26 ppm, or  $\text{H}_2\text{O}$  at 4.79 ppm;  $^{13}\text{C}$ :  $\text{DMSO-}d_5$  at 39.52 ppm and  $\text{CHCl}_3$  at 77.16 ppm. Peak deconvolution was performed by applying a quantitative global spectrum deconvolution method (GSD) with 20 fitting cycles (refinement level 4) and 10 improvement cycles.

DOSY NMR experiments were conducted on a Bruker Avance DRX (500 MHz) and the spectra recorded with 64 scans. The relaxation delay (D1) and the gradient recovery delay were kept fixed at 3 s and 0.2 ms, respectively. The strength of the pulsed-field gradients was increased from 2% to 98% of the maximal gradient strength (10 A) in 16 steps, whereas the diffusion-sensitive period ( $\Delta$ ) was set to 0.06 s and the gradient duration ( $\delta$ ) was set to 2 ms. The obtained data were processed with MestreNova by applying a DOSY transform (Bayesian method). ROESY NMR experiments were performed on a Bruker Avance DRX (500 MHz) with a pulse spin lock of 200 ms.

**Electrospray ionization-mass spectrometry (ESI-MS).** ESI experiments were recorded on a Q-Exactive (Orbitrap) mass spectrometer (Thermo Fisher Scientific, San Jose, CA, USA) equipped with a HESI II probe. Formic acid was added to selected samples to improve ionizability. The spectra were interpreted by peaks of protonated molecules  $[\text{M} + \text{H}]^+$  and adducts such as  $[\text{M} + \text{NH}_4]^+$  or  $[\text{M} + \text{Na}]^+$ . All peaks are indicated with their mass-to-charge ratio ( $m/z$ ).

**Differential scanning calorimetry (DSC).** DSC measurements were performed on a Mettler Toledo DSC 3 (Greifensee, Canton



of Zurich, Switzerland) using a Huber Intracooler TC100 (Offenburg, Baden-Württemberg, Germany) and aluminum crucibles (40.0  $\mu\text{L}$ ). The experiments were performed under nitrogen flow (50 mL  $\text{min}^{-1}$ ) in two consecutive heating-cooling cycles:  $-20$ – $300$   $^{\circ}\text{C}$ ,  $300$  to  $-20$   $^{\circ}\text{C}$  and  $-20$ – $300$   $^{\circ}\text{C}$  at a heating/cooling rate of  $10$  K  $\text{min}^{-1}$ . Each measurement was performed using 3–7 mg of substance.

**Thermogravimetric analysis (TGA).** Thermogravimetric measurements were performed on a TGA Q5500 instrument (New Castle, DE, USA) from TA Instruments. The samples were dried under reduced pressure (10 mbar) at  $65$   $^{\circ}\text{C}$  overnight before each measurement. The samples (3–7 mg) were heated in a platinum crucible in the range of  $25$ – $800$   $^{\circ}\text{C}$  under a nitrogen atmosphere at a heating rate of  $10$  K  $\text{min}^{-1}$ .  $T_{d,5\%}$  is defined as the temperature at which 5% weight loss of the sample occurred, while  $T_{d,50\%}$  is defined as the temperature at which 50% of the weight loss of the sample was detected.

**Size exclusion chromatography (SEC).** SEC measurements were performed on an Agilent Technologies 1260 Infinity II (Waldbronn, Baden-Württemberg, Germany) equipped with a Mixed-C  $5$   $\mu\text{m}$  and Mixed-E  $3$   $\mu\text{m}$  Agilent column, and a differential refractive index detector. The used eluent was DMAc containing  $0.034$  wt% LiBr. The number average molar mass ( $M_n$ ), the weight average molar mass ( $M_w$ ), and the dispersity ( $D = M_w/M_n$ ) of the samples were determined using a calibration of poly(methyl methacrylate) (PMMA) standards ranging from  $800$  to  $2.2 \times 10^6$  Da. The samples were dissolved in the eluent at a concentration of  $2$  mg  $\text{mL}^{-1}$  and filtered over a  $0.2$   $\mu\text{L}$  filter.

**Inductively coupled plasma optical emission spectrometry (ICP-OES).** ICP-OES measurements were performed on an ICP-OES iCap 7000 (Thermo Fisher Scientific, Waltham, MA, USA). For the sample preparation,  $5$  mg of the analyte were treated with a mixture of 68% nitric acid and 30% hydrogen peroxide in a digitube and heated in a DigiPREP heating system for 2 h. Afterwards, the liquid was evaporated and diluted with deionized water up to  $20$  mL. All measurements were conducted in duplicates to minimize the susceptibility to errors.

## Conflicts of interest

The authors declare no conflict of interest.

## Data availability

The data supporting this article have been included as part of the SI.

Supplementary information is available. See DOI: <https://doi.org/10.1039/d5su00590f>.

## Acknowledgements

This project was kindly supported by Eucor – The European Campus (project: Smart functional sequence-defined oligomers and polymers incorporating rigid cyclodextrin host molecules). The authors gratefully acknowledge the financial support provided to P. Conen by the Graduate funding of the German

States. The authors acknowledge support by the state of Baden-Württemberg through bwHPC and the German Research Foundation (DFG) through grant no INST 40/575-1 FUGG (JUSTUS 2 cluster). The authors would like to thank the working group of Prof. Théato for the assistance during the TGA and SEC measurements, Dr Jonas Wenzel for the supply of GaBr<sub>3</sub>, and Dr Elisabeth Eiche for performing ICP-OES measurements.

## References

- 1 N. Morin-Crini, S. Fourmentin, É. Fenyvesi, E. Lichtfouse, G. Torri, M. Fourmentin and G. Crini, *Environ. Chem. Lett.*, 2021, **19**, 2581–2617.
- 2 M. L. Bender and M. Komiyama, *Cyclodextrin Chemistry*, Springer Science & Business Media, 2012.
- 3 J. Szejtli, *Chem. Rev.*, 1998, **98**, 1743–1754.
- 4 M. E. Brewster and T. Loftsson, *Adv. Drug. Deliv. Rev.*, 2007, **59**, 645–666.
- 5 G. Crini, *Chem. Rev.*, 2014, **114**, 10940–10975.
- 6 P. Anastas and N. Eghbali, *Chem. Soc. Rev.*, 2010, **39**, 301–312.
- 7 M. E. Davis and M. E. Brewster, *Nat. Rev. Drug Discovery*, 2004, **3**, 1023–1035.
- 8 M. Petitjean, I. X. Garcia-Zubiri and J. R. Isasi, *Environ. Chem. Lett.*, 2021, **19**, 3465–3476.
- 9 S. Payamifar and A. Poursattar Marjani, *Appl. Organomet. Chem.*, 2023, **37**, e7287.
- 10 Y. Liu, D. E. Sameen, S. Ahmed, Y. Wang, R. Lu, J. Dai, S. Li and W. Qin, *Food Chem.*, 2022, **370**, 131026.
- 11 Q. Liu, Y. Zhou, J. Lu and Y. Zhou, *Chemosphere*, 2020, **241**, 125043.
- 12 E. M. M. Del Valle, *Process Biochem.*, 2004, **39**, 1033–1046.
- 13 L. Jicsinszky and J. Szejtli, *Effect of catalysts on the acylation of cyclodextrins*, 1992.
- 14 L. Jicsinszky, K. Martina, M. Caporaso, P. Cintas, A. Zanichelli and G. Cravotto, *Phys. Chem. Chem. Phys.*, 2015, **17**, 17380–17390.
- 15 Z.-T. Liu, L.-H. Shen, Z.-W. Liu and J. Lu, *J. Mater. Sci.*, 2009, **44**, 1813–1820.
- 16 D. Yu, K. Steffensen, J. Tranholm, A. L. Nielsen, R. Wimmer, K. L. Larsen and J. Incl, *J. Inclusion Phenom. Macrocyclic Chem.*, 2007, **57**, 333–338.
- 17 H. Held, A. Rengstl and D. Mayer, in *Ullmann's Encyclopedia of Industrial Chemistry*, 2000, DOI: [10.1002/14356007.a01\\_065](https://doi.org/10.1002/14356007.a01_065).
- 18 F. Bienewald, E. Leibold, P. Tužina and G. Roscher, in *Ullmann's Encyclopedia of Industrial Chemistry*, 2019, pp. 1–16, DOI: [10.1002/14356007.a27\\_419.pub2](https://doi.org/10.1002/14356007.a27_419.pub2).
- 19 J. Wolfs and M. A. R. Meier, *Green Chem.*, 2021, **23**, 4410–4420.
- 20 D. Mathiron, F. Marcon, J. M. Dubaele, D. Cailleu, S. Pilard and F. Djedaini-Pilard, *J. Pharm. Sci.*, 2013, **102**, 2102–2111.
- 21 T. Loftsson and D. Duchene, *Int. J. Pharm.*, 2007, **329**, 1–11.
- 22 J. Szejtli and J. Inclusion Phenom, *J. Inclusion Phenom. Mol. Recognit. Chem.*, 1992, **14**, 25–36.
- 23 T. Loftsson and M. E. Brewster, *J. Pharm. Sci.*, 1996, **85**, 1017–1025.



- 24 X. Cai, W. Liu and S. Chen, *J. Agric. Food Chem.*, 2005, **53**, 6744–6749.
- 25 J. Jindrich, J. Pitha, B. Lindberg, P. Seffers and K. Harata, *Carbohydr. Res.*, 1995, **266**, 75–80.
- 26 M. Řezanka, *Environ. Chem. Lett.*, 2018, **17**, 49–63.
- 27 J. Szejtli, A. Liptak, I. Jodal, P. Fügedi, P. Nanasi and A. Neszmelyi, *Starch/Staerke*, 1980, **32**, 165–169.
- 28 A. G. Molina, V. Kungurtsev, P. Virta and H. Lonnberg, *Molecules*, 2012, **17**, 12102–12120.
- 29 A. R. Khan, P. Forgo, K. J. Stine and V. T. D'Souza, *Chem. Rev.*, 1998, **98**, 1977–1996.
- 30 R. A. Sheldon, *Green Chem.*, 2007, **9**, 1273–1283.
- 31 R. A. Sheldon, *Green Chem.*, 2016, **18**, 3180–3183.
- 32 U. Biermann and J. O. Metzger, *Eur. J. Lipid Sci. Technol.*, 2013, **116**, 74–79.
- 33 U. Biermann and J. O. Metzger, *ChemSusChem*, 2014, **7**, 644–649.
- 34 P. K. Dannecker, U. Biermann, M. von Czapiewski, J. O. Metzger and M. A. R. Meier, *Angew Chem. Int. Ed. Engl.*, 2018, **57**, 8775–8779.
- 35 M. Rhein, S. Zorbakhsh and M. A. R. Meier, *Macromol. Chem. Phys.*, 2022, **224**, 2200289.
- 36 H. Chen, F. Yang, J. Du, H. Xie, L. Zhang, Y. Guo, Q. Xu, Q. Zheng, N. Li and Y. Liu, *Cellulose*, 2018, **25**, 6935–6945.
- 37 D. Prat, J. Hayler and A. Wells, *Green Chem.*, 2014, **16**, 4546–4551.
- 38 A. W. T. King, J. Jalomäki, M. Granström, D. S. Argyropoulos, S. Heikkinen and I. Kilpeläinen, *Anal. Methods*, 2010, **2**, 1499–1505.
- 39 J. Pesti and G. L. Larson, *Org. Process Res. Dev.*, 2016, **20**, 1164–1181.
- 40 N. Sakai, T. Moriya, K. Fujii and T. Konakahara, *Synthesis*, 2008, **2008**, 3533–3536.
- 41 F. G. Delolo, E. N. dos Santos and E. V. Gusevskaya, *Green Chem.*, 2019, **21**, 1091–1098.
- 42 C. M. Alder, J. D. Hayler, R. K. Henderson, A. M. Redman, L. Shukla, L. E. Shuster and H. F. Sneddon, *Green Chem.*, 2016, **18**, 3879–3890.
- 43 N. Sakai, T. Moriya and T. Konakahara, *J. Org. Chem.*, 2007, **72**, 5920–5922.
- 44 T. El Achkar, T. Moufawad, S. Ruellan, D. Landy, H. Greige-Gerges and S. Fourmentin, *Chem. Commun.*, 2020, **56**, 3385–3388.
- 45 Y. Zhang, S. Yu and F. Bao, *Carbohydr. Res.*, 2008, **343**, 2504–2508.
- 46 M. J. Frisch, G. W. Trucks, H. B. Schlegel, G. E. Scuseria, M. A. Robb, J. R. Cheeseman, G. Scalmani, V. Barone, G. A. Petersson, H. Nakatsuji, X. Li, M. Caricato, A. V. Marenich, J. Bloino, B. G. Janesko, R. Gomperts, B. Mennucci, H. P. Hratchian, J. V. Ortiz, A. F. Izmaylov, J. L. Sonnenberg, D. Williams-Young, F. Ding, F. Lipparini, F. Egidi, J. Goings, B. Peng, A. Petrone, T. Henderson, D. Ranasinghe, V. G. Zakrzewski, J. Gao, N. Rega, G. Zheng, W. Liang, M. Hada, M. Ehara, K. Toyota, R. Fukuda, J. Hasegawa, M. Ishida, T. Nakajima, Y. Honda, O. Kitao, H. Nakai, T. Vreven, K. Throssell, J. A. Montgomery Jr, J. E. Peralta, F. Ogliaro, M. J. Bearpark, J. J. Heyd, E. N. Brothers, K. N. Kudin, V. N. Staroverov, T. A. Keith, R. Kobayashi, J. Normand, K. Raghavachari, A. P. Rendell, J. C. Burant, S. S. Iyengar, J. Tomasi, M. Cossi, J. M. Millam, M. Klene, C. Adamo, R. Cammi, J. W. Ochterski, R. L. Martin, K. Morokuma, O. Farkas, J. B. Foresman and D. J. Fox, *Gaussian 16, Revision C.01*, 2016.

